ON THE DESIGN OF SMALL COARSE SPACES FOR DOMAIN DECOMPOSITION ALGORITHMS

CLARK R. DOHRMANN * AND OLOF B. WIDLUND †

TR2017-987

Abstract. Methods are presented for automatically constructing coarse spaces of low dimension for domain decomposition algorithms. These constructions use equivalence classes of nodes on the interface between the subdomains into which the domain of a given elliptic problem has been subdivided, e.g., by a mesh partitioner such as METIS; these equivalence classes already play a central role in the design, analysis, and programming of many domain decomposition algorithms. The coarse space elements are well defined even for irregular subdomains, are continuous, and well suited for use in two-level or multi-level preconditioners such as overlapping Schwarz algorithms. An analysis for scalar elliptic and linear elasticity problems reveals that significant reductions in the coarse space dimension can be achieved while not sacrificing the favorable condition number estimates for larger coarse spaces previously developed. These estimates depend primarily on the Lipschitz parameters of the subdomains. Numerical examples for problems in three dimensions are presented to illustrate the methods and to confirm the analysis. In some of the experiments, the coefficients have large discontinuities across the interface between the subdomains, and in some, the subdomains are generated by mesh partitioners.

Key words. elliptic equations, linear elasticity, domain decomposition methods, two-level overlapping Schwarz preconditioners, small coarse spaces, finite elements

AMS subject classifications. 65F08, 65F10, 65N30, 65N55

1. Introduction.

Coarse spaces are at the heart of many domain decomposition algorithms. Building on the foundation laid in [18], we have an ongoing interest in the development of coarse spaces based on energy minimization concepts begun in [9]. Several different problem classes have been studied in recent years, including compressible and almost incompressible elasticity, [11, 12], problems in $H(div)$, [32], and two-dimensional problems with subdomains with irregular shapes, [10, 25], including problems in $H(\mathbf{curl})$, [6, 7, 14]. We also note that there has been much complementary work to address problems with multiple materials inside individual subdomains over the last decade, see, e.g., [19, 21].

The purpose of this study, which is a substantial extension of a conference paper, [15], is to develop and study a family of low dimensional coarse spaces for scalar elliptic and elasticity problems. We will focus on problems in three dimensions. The basic idea involves the use of certain equivalence classes of nodes on the interface, i.e., nodes that belong to more than one subdomain boundary. Subdomain faces, edges, and vertices can easily be defined in terms of equivalence classes of finite element nodes on the interface between subdomains. Coarse degrees of freedom are then associated with some of these classes and the coarse basis functions are obtained from discrete harmonic, energy minimizing extensions of Dirichlet data given on the subdomain boundaries. For a domain partitioned into subdomains with vertices in the interior of the domain, the equivalence classes relevant to the coarse basis functions are simply

*Computational Solid Mechanics and Structural Dynamics Department, Sandia National Laboratories, Albuquerque, New Mexico, 87185 crdohrm@sandia.gov. Sandia is a multiprogram laboratory operated by Sandia Corporation, a Lockheed Martin Company, for the United States Department of Energy's National Nuclear Security Administration under Contract DE-AC04-94-AL85000.

†Courant Institute of Mathematical Sciences, 251 Mercer Street, New York, NY 10012, USA widlund@cims.nyu.edu, http://cs.nyu.edu/cs/faculty/widlund/index.html. The work of this author was supported in part by the National Science Foundation Grant DMS-1522736.

defined in terms of one degree of freedom for a scalar elliptic problem and six for linear elasticity for each such vertex.

Our analysis for scalar elliptic and linear elasticity problems will reveal that significant reductions in the coarse space dimension can often be achieved without sacrificing the favorable condition number estimates for larger coarse spaces. This can be important when the memory and computational requirements associated with larger coarse spaces are prohibitive due to the use of large numbers of processors on a parallel computer. A multi-level approach could be used in such cases, but this may not always be the best possible solution. In addition, smaller coarse spaces are likely to become more important as future computing architectures move to less memory per core [1]. Algorithms like those in this study have been applied to linear systems originating from large scale structural dynamics analyses [34].

We are principally concerned with overlapping Schwarz methods in this paper, but our new coarse spaces can also replace the coarse spaces of many of the iterative substructuring algorithms of [36, Chapter 5]. We note that the overlapping Schwarz algorithms have the advantage that they are well defined for problems for which only the assembled stiffness matrix is available while many other domain decomposition algorithms require knowledge of the matrices that represent the contribution of individual subdomains to the system.

We note that an earlier study on FETI–DP algorithms for compressible elasticity in three dimensions, [27], had a similar purpose of eliminating as many *primal constraints* as possible while maintaining the best possible bounds for the convergence rate of the algorithm. We note that the primal constraints define the global, coarse space component for this class of domain decomposition algorithms. In the final subsection of that paper, a relatively complicated recipe is provided which reduces the dimension of the primal space to about six times the number of subdomains; the well-known null space property, cf. [35, p. 132], shows that this indeed is about the minimum given that the six rigid body modes span the null space of the elasticity operator.

The development of theory for domain decomposition algorithms has often focused on issues related to large discontinuities of the coefficient. Thus, for iterative substructuring algorithms, based on non-overlapping subdomains, a number of results have been developed for elliptic problems where the coefficients are constant or vary slowly inside the subdomains but without any restrictions on their variation across the interface between the subdomains; see, e.g., [36, Chapters 4–6] and [27]. Many of these algorithms are well-defined for arbitrary subdomains although the theory has been fully developed mostly for subdomains that are tetrahedral or the unions of a few large tetrahedra. In contrast, the theory for two–level additive Schwarz methods is developed only for constant coefficients in Chapter 3 of the same monograph. However, the classical coarse spaces for these Schwarz algorithms have been shown to be stable for *quasi–monotone* coefficients in [17]; for a related condition, see Assumption 1 of this paper. The result in [17] considerably expanded the class of subdomain coefficients for which results quite similar to those for constant coefficients became possible. This was followed by a number of studies of problems with large variations of the coefficients inside the subdomains, see, e.g., [20] and [37]. In all this work, the main focus is on the construction and analysis of the coarse spaces. A recent paper, [28], is focused on handling irregular subdomains and effective massively parallel computing.

We note that the issue on the effects of jumps in the coefficients across the interface is closely related to bounds for weighted L^2-projections as considered in [2]

and [38]. A counterexample for three dimensions, given in the latter paper, involves a number of subdomains which have a subdomain vertex in common; two of the subdomains have only that vertex in common and they are surrounded by subdomains with much smaller diffusion coefficients. In this paper, we are able to relax the condition of [17] for scalar elliptic problems; cf. Assumption 2. For linear elasticity, more stringent conditions, similar to those of [17], will be required; see Assumption 1. We have experimental evidence that the elasticity problems indeed require a stronger assumption; see Table 6. While we are unable to handle coefficients as in the counterexample of [38], we are able to include the well-known case of three-dimensional checker-board distributions for scalar elliptic problems. Thus, we are able to partially close the gap in the theory between the assumptions on the coefficients that have existed between the iterative substructuring algorithms and overlapping Schwarz algorithms with all of their coarse space elements tied to subdomain vertices. We note that we could eliminate these assumptions on the coefficients by expanding the coarse space by basis functions related to subdomain edges as in [12]. We also note that the use of additional basis functions related to subdomain faces instead of edges is likely to require some assumptions on the coefficients of the subdomains; see [24, 26] for a discussion of FETI–DP algorithms primarily using face constraints.

Results similar to those of [12] have recently been developed for almost incompressible elasticity in [4, 5] where the coarse space is a conventional one based on a coarse triangulation of Ω; the Lamé parameter μ is essentially assumed to meet the requirements of Assumption 1 of this paper. In contrast to the algorithm of those studies, the coarse spaces of this study are also well defined for quite arbitrary subdomains generated, e.g., by a mesh partitioner. In our analysis, we have focused on the compressible case but we have found in numerical experiments, reported in Table 8, that our algorithm appears to be viable even when we approach the incompressible limit. We note that in our earlier work, [12], we have enriched our coarse spaces by adding a coarse degree of freedom for each subdomain face in the almost incompressible case; we also report on numerical results with such enlarged coarse spaces.

To derive our final bounds for our domain decomposition algorithms, we also need to consider the components associated with local problems defined on overlapping subdomains, Ω_i', which are often constructed by extending nonoverlapping subdomains, Ω_i, into which the given domain Ω, has been decomposed, by adding one or a few layers of elements. Here no new ideas are required for a complete analysis; cf. [36, Subsection 3.2] and the discussion in [13, Section 3]. Therefore, in this paper, we will focus on developing new coarse spaces and on establishing bounds for the coarse component, which are always required in the analysis of any Schwarz algorithm; see [36, Subsection 2.3].

In the next section, we describe the nodal equivalence classes that are used in the construction of the coarse spaces. Algorithms for generating the coarse basis functions for different problem types are provided in Section 3. An analysis for scalar elliptic equations is given in Section 4. In Section 5, the equations of linear elasticity and Korn inequalities are introduced, and in Section 6 condition number bounds are developed for that case. Finally, numerical examples are presented in Section 7.

2. Nodal Equivalence Classes and Coarse Nodes. We will focus on three-dimensional elliptic problems approximated by nodal, low order, Lagrangian finite element methods and we will consider a domain Ω partitioned into non-overlapping subdomains $\Omega_1, \ldots, \Omega_N$. The subdomains, which are unions of elements, that form

quasi–uniform meshes for each subdomain, will often have irregular boundaries, in particular, if they have been generated by a mesh partitioner. Some of the tools used in our analysis, such as a trace theorem, will require that the subdomains are Lipschitz. The interface set of points common to two or more subdomain boundaries is denoted by Γ and the local interface set of a subdomain boundary Ω_i is denoted by $\Gamma_i := \Gamma \cap \partial\Omega_i$. We will also, at times, work with all nodes on the subdomain boundaries $\partial\Omega_i$.

Let $\mathcal{S}_n$ denote the index set of the subdomains with node n on their boundaries. Two nodes n_j, n_k are equivalent if $\mathcal{S}_{n_j} = \mathcal{S}_{n_k}$. As for FETI-DP or BDDC methods, we partition Γ into *nodal equivalence classes* based on this equivalence relation. In fact, we will also work with equivalence classes of nodes on $\partial\Omega$. Thus, we have a nodal equivalence class associated with each subdomain face; for an interior face it is given by a set of nodes shared by just two subdomain boundaries. Similarly, we have an equivalence class associated with each subdomain edge – a set of nodes on part of the boundaries of faces and typically shared by three or more subdomains – and an equivalence class with only one element associated with each subdomain vertex located at the end of edges and typically shared by even more subdomains. For economy of words, we will henceforth use the abbreviation *nec* for nodal equivalence class.

Let $\mathcal{S}_{\mathcal{N}}$ denote the index set of subdomains for any node of *nec* $\mathcal{N}$. A *nec* $\mathcal{N}_j$ is said to be an *offspring* of *nec* $\mathcal{N}_k$ if $\mathcal{S}_{\mathcal{N}_j} \subset \mathcal{S}_{\mathcal{N}_k}$. Likewise, $\mathcal{N}_k$ is called an *ancestor* of $\mathcal{N}_j$ in this case. A *nec* is designated a *coarse node* if it is not the offspring of any other *nec*.

Let $\mathcal{M}_i$ denote the set of all *necs* of Ω_i. We note that each *nec* in $\mathcal{M}_i$ is either a coarse node or the offspring of at least one coarse node. Further, a coarse node c of Ω_i is also a coarse node of Ω_j for all $j \in \mathcal{S}_c$.

We note that for a decomposition into N cubic subdomains, the coarse nodes are the subdomain vertices. If all *necs* are used directly in the construction of coarse basis functions, as in [9], then there will be approximately $(6/2 + 12/4 + 8/8)N = 7N$ *necs* associated with the coarse space. Likewise, if only subdomain edges and vertices are used, for this purpose, as in [12], then there are approximately $(12/4 + 8/8)N = 4N$ such *necs*. In contrast, the coarse space of this study is based on only about N coarse nodes. We note that subdomain vertex nodes have the advantage of being shared by more subdomains than subdomain edges and faces.

For linear elasticity, we will use six degrees of freedom for each coarse node. For a domain subdivided into cubes, each interior subdomain vertex is shared by eight subdomains and since the number of such subdomain vertices for a single subdomain also equals eight, the number of coarse degrees of freedom contributed by a subdomain will then equal six, the dimension of the space of rigid body modes attributed to a subdomain.

But there are also other cases which can be made part of our framework, some of which are quite simple to describe. Thus if our domain is just the union of two subdomains that share a face, then there is just one coarse node associated with that face. We note that such a pair of subdomains could also belong to a larger set of subdomains. On the other hand if there are only three subdomains which have an edge in common, in addition to faces that are shared by only pairs of them, then the coarse node is represented by that edge. However, our analysis will be confined to the case when the coarse degrees of freedom are associated with subdomain vertices.

3. Coarse Basis Functions. In this section, we describe how to construct coarse basis functions for scalar elliptic and elasticity problems in three dimensions.

The support of a coarse basis function associated with the coarse node c will be the union of the closure of all Ω_j with $j \in \mathcal{S}_c$. The coarse basis functions will be continuous across subdomain interfaces and we can therefore focus on a single subdomain Ω_i.

The first step is to obtain a partition of unity for the nodes on $\partial\Omega_i$. Let $\mathcal{C}_\mathcal{N}$ denote the set of ancestor coarse nodes for *nec* $\mathcal{N}$. If $\mathcal{N}$ is itself a coarse node, we then take $\mathcal{C}_\mathcal{N} = \mathcal{N}$. For the simplest case, the partition of unity associated with a node $n \in \mathcal{N}$ and a coarse node $c \in \mathcal{C}_\mathcal{N}$ is chosen as

$$p_{nc} = 1/|\mathcal{C}_\mathcal{N}|. \tag{1}$$

One can easily confirm that $\sum_{c\in\mathcal{C}_\mathcal{N}} p_{nc} = 1$. We will refer to this choice as *Option 1*.

We note from (1) that p_{nc} is the same for all $n \in \mathcal{N}$ and $c \in \mathcal{C}_\mathcal{N}$; in the case of tetrahedral subdomains, the basis functions constructed will be built from the face and edge functions, $\theta_\mathcal{F}$ and $\theta_\mathcal{E}$, used extensively in the development of iterative substructuring algorithms as in [36, Chapters 4-6]; see also Lemmas 1 and 2. This feature causes large changes in the coarse basis functions across *nec* boundaries, resulting in a logarithmic factor $(1 + \log(H_i/h_i))$ in our estimate of the energy of the coarse basis functions; cf. [36, Lemma 4.25] for a bound of the energy of the classical face function $\theta_\mathcal{F}$. Here, H_i is the diameter of Ω_i and h_i is the diameter of its smallest element. We will show that we can obtain the same quality bound for Lipschitz subdomains by providing generalizations of the bounds for the face and edge functions for subdomains assumed only to be Lipschitz; see Lemmas 1 and 2.

In an attempt to avoid such a logarithmic factor, we will also consider a partition of unity originating from linear functions rather than constants; it will be easy to see that we will have success for a subdomain that is a tetrahedron. Define

$$a(n) := \begin{bmatrix} 1 & x_{n1} & x_{n2} & x_{n3} \end{bmatrix},$$

where x_{nj} is the j-coordinate of node n. Let the matrix $A_\mathcal{N}$ denote the row concatenation of the $a(n)$ for all coarse nodes in $\mathcal{C}_\mathcal{N}$. We note that the number of rows of $A_\mathcal{N}$ equals the number of ancestor coarse nodes for $\mathcal{N}$ and that there are four columns. Here the origin of the local coordinate system is chosen as the centroid of the ancestor coarse nodes of $\mathcal{C}_\mathcal{N}$. With reference to (1), p_{nc} is now chosen as

$$p_{nc} = a(n)A^\dagger_\mathcal{N} e_c, \tag{2}$$

where $A^\dagger_\mathcal{N}$ is the Moore-Penrose pseudo-inverse and e_c a column vector with a single nonzero entry of 1 in the row of $A_\mathcal{N}$ corresponding to the coarse node c. We note that if $a(n)$ is replaced by only its first element, then (2) simplifies to (1). We also note that there can be complications when the rows of $A_\mathcal{N}$ are linearly or almost linearly dependent; for the time being, we will first ignore this fact but will return to this issue at the end of this section.

We now show, by using standard results on Moore-Penrose pseudo-inverses, that $\sum_{c\in\mathcal{C}_\mathcal{N}} p_{nc} = 1$ in case the number of rows of $A_\mathcal{N}$ is 4 or more: Consider a linear system of the form $A_\mathcal{N} x = b$, where $b = (1, \ldots, 1)^T$. We find that the solution is $(1, 0, 0, 0)^T$ given that the first element of each of the rows of $A_\mathcal{N}$ equals 1. The inner product of $a(n)$ and x will therefore always equal 1.

For the case when the number of rows of $A_\mathcal{N}$ are only 3, we find that the same x is a solution, but in order to show that this is the minimal norm solution provided by the Moore-Penrose pseudo-inverse, we need to show that $(1, 0, 0, 0)^T$ is orthogonal to

all elements in the null space of $A_{\mathcal{N}}$, which in this case has dimension 1. We therefore consider the 3−by−3 matrix obtained from the second, third, and fourth columns of $A_{\mathcal{N}}$. Since the sum of the rows of this matrix vanishes, by the choice of the coordinate system, we can find a nontrivial null vector $\hat{n}$, which we augment with a leading 0. The resulting vector is clearly in the null space of $A_{\mathcal{N}}$ and it is also orthogonal to $(1,0,0,0)^T$.

The case when there are fewer than 3 rows of $A_{\mathcal{N}}$ can be handled quite similarly; we can find the right number of linearly independent null vectors with a leading 0. Thus, we always find that $\sum_{c\in C_{\mathcal{N}}} p_{nc} = 1$ and that we have a partition of unity.

The energy associated with a finite element function over Ω_i is defined as $E_i(u^{(i)}) := u^{(i)T} A^{(i)} u^{(i)}$, where $u^{(i)}$ is a vector of nodal degrees of freedom (*dofs*) of the closure of Ω_i and $A^{(i)}$ the stiffness matrix for Ω_i. Let $R_n^{(i)}$ select the rows of $u^{(i)}$ for the dofs of node $n \in \mathcal{N}$, i.e., $R_n^{(i)} u^(i)$ is the vector of dofs for node n; in the case of a scalar elliptic problem, there will be only one element, while for elasticity, there will be three. Let $\mathcal{N}_c^{(i)}$ denote the set of nodes on $\partial\Omega_i$, which have c as an ancestor coarse node and define

$$\Psi_{ic} := \sum_{n\in\mathcal{N}_c^{(i)}} p_{nc} {R_n^{(i)}}^T N_{nc}, \tag{3}$$

where the matrix N_{nc} is specified later for different problem types.

Let $R_B^{(i)}$ and $R_I^{(i)}$ select the rows of $u^{(i)}$ for the nodal dofs on $\partial\Omega_i$ and the interior of Ω_i, respectively, and define

$$A_{BB}^{(i)} := R_B^{(i)} A^{(i)} {R_B^{(i)}}^T, \quad A_{IB}^{(i)} := R_I^{(i)} A^{(i)} {R_B^{(i)}}^T, \quad A_{II}^{(i)} := R_I^{(i)} A^{(i)} {R_I^{(i)}}^T.$$

The coarse basis function associated with the coarse node c is given by

$$\Phi_{ic} = \Psi_{ic} - {R_I^{(i)}}^T {A_{II}^{(i)}}^{-1} A_{IB}^{(i)} (R_B^{(i)} \Psi_{ic}).$$

We note that the first term on the right hand side of this expression represents the boundary data for the coarse basis function, while the second term represents its energy-minimizing extension into the interior of Ω_i.

For scalar elliptic equations, like the Poisson equation, we choose

$$N_{nc} = \begin{bmatrix} 1 \end{bmatrix}.$$

For elasticity problems in three dimensions, N_{nc} is chosen as

$$N_{nc} = \begin{bmatrix} 1 & 0 & 0 & 0 & x_{n3}^c & -x_{n2}^c \\ 0 & 1 & 0 & -x_{n3}^c & 0 & x_{n1}^c \\ 0 & 0 & 1 & x_{n2}^c & -x_{n1}^c & 0 \end{bmatrix}, \tag{4}$$

where x_{nj}^c is the j-coordinate of node n. We will assume that the origin of the coordinate system is chosen as the centroid of the relevant coarse nodes. The first three columns of N_{nc} correspond to rigid body translations, while the final three columns correspond to rigid body rotations about the origin. We will denote these six column vectors by $\boldsymbol{r}_i, i = 1, 2, \ldots, 6$. We note that the expression for N_{nc} can be adapted easily to accommodate finite element models with shell elements simply by adding three more rows to N_{nc}.

It is easy to see that the energy of basis functions originating from the formula (2) will depend primarily on the norm of $A_{\mathcal{N}}^{\dagger}$. If there are four ancestor coarse nodes that lie in a plane, then there will be one zero singular value and if one of these nodes is moved slightly off the plane, there will be a small singular value and $A_{\mathcal{N}}^{\dagger}$ will have a large norm. We will therefore explore an alternative recipe for the construction of the coarse basis functions. For the case of four coarse nodes, let $d_i(n), i = 1, \ldots, 4$, be the distance between a node $n \in \mathcal{N}$ on the face and c_i, the ith ancestor coarse node. We then assign the values

$$p_{nc_i} := \frac{1/d_i(n)}{1/d_1(n) + 1/d_2(n) + 1/d_3(n) + 1/d_4(n)} \tag{5}$$

to the node n. We note that not only do these functions take values in the interval $[0, 1]$ but by a simple computation, we also find that their gradients are bounded by C/H_i. As a consequence, we can derive the same quality bound for the energy of the resulting coarse basis functions; cf. (6). In our experiments with *Option 2*, we will use formula (2) for all cases when there are three or fewer ancestor nodes and formula (5) otherwise.

This approach resembles *inverse distance weighting*, a technique used for multivariate interpolation of data on a scattered set of points originating with [33]. However, our context appears to be quite different from that work. We note that we apply the formula (5) only for a few coarse nodes at a time and that we use it only to generate values at the nodes on the interface while the values in the interior of the subdomains are provided by discrete harmonic extensions.

REMARK 1. *The coarse space in [10], a study of two-dimensional problems, is obtained by choosing the subdomain vertices and edges as the coarse nodes, and using the partition of unity given in (1). In contrast, the smaller coarse space of [13] is obtained by choosing only the subdomain vertices as the coarse nodes and using a partition of unity similar to the one given by (2). The algorithm with the smaller coarse space was found to converge faster than the one with the larger coarse space. Both these earlier papers concern problems in two dimensions and we were able to develop a theory for quite irregular subdomains, which are only uniform in the sense of Peter Jones, [22]. We note that the uniform domains include domains with fractal boundaries and that an extension theorem holds for any uniform domain; for two dimensions, it is a sufficient as well as necessary condition. The technical difficulties for three-dimensional problems are more severe and we have, so far, had to confine our study to Lipschitz subdomains.*

4. Analysis of the Scalar Case. As pointed out at the end of section 2, our framework can be used for coarse nodes which are not associated with subdomain vertices, but our analysis will be restricted to that case. In this section, we develop estimates for the energy of a coarse interpolant of $u^{(i)}$ for a scalar elliptic equation: find $u \in H_0^1(\Omega)$, such that

$$a(u, v) = f(v) \quad \forall v \in H_0^1(\Omega, \partial\Omega),$$

where

$$H_0^1(\Omega) := \{v \in H^1(\Omega) : v = 0 \ \ on \ \ \partial\Omega\},$$

and where

$$a(u, v) := \int_\Omega \rho(x) \nabla u \cdot \nabla v dx \ \ and \ \ f(v) := \int_\Omega f v dx.$$

The diffusion coefficient $\rho(x) > 0$ is assumed to take on a constant value ρ_i in Ω_i. We will use the symbol $u^{(i)}$ for both a finite element function and its vector representation in terms of nodal values in the closure of Ω_i. Similarly, ϕ_{ic} is the finite element function counterpart of Φ_{ic}.

The case of shape-regular tetrahedral subdomains is particularly simple. In this case, the coarse basis functions for Ω_i based on (2) are identical to those for the standard P_1 linear tetrahedral element on $\partial\Omega_i$. Consequently, the coarse basis functions are also identical to the standard shape functions throughout Ω_i since a linear function minimizes the energy for boundary data given by a linear function. We then have the standard estimate

$$E_i(\phi_{ic}) \leq CH_i\rho_i. \tag{6}$$

for Option 2.

This bound also holds for general Lipschitz subdomains for coarse basis functions defined by (2): Let us first dilate the subdomain so that its diameter equals 1. The gradient of any basis function can then be shown to have a constant, uniformly bounded gradient. The result then follows by returning to the original coordinates.

The same bound also holds for coarse basis functions obtained by using (5) since as we have already pointed out, the gradient of these functions are bounded by C/H_i.

For the case when the partition of unity is chosen as in (1), i.e., for Option 1, as well as in some other arguments, we need two auxiliary results which are well known for tetrahedra. We recall that we already have noticed that in this case a coarse basis function can be written as a linear combination of face and edge functions as defined in Lemmas 1 and 2.

LEMMA 1. *(face function) Let $\mathcal{F}$ be a face of a Lipschitz domain Ω_i and define a finite element function $\theta_{\mathcal{F}}$ which equals 1 at all nodes on $\mathcal{F}$, vanishes at all other nodes of $\partial\Omega_i$, and which is discrete harmonic, i.e., has the minimum $H^1(\Omega_i)-$semi-norm of all functions with this Dirichlet data. Then,*

$$|\theta_{\mathcal{F}}|^2_{H^1(\Omega_i)} \leq CH_i(1 + \log(H_i/h_i)).$$

Here C is a constant.

This is [8, Lemma 4.7].

We need a similar result for subdomain edges.

LEMMA 2. *(edge function) Let $\mathcal{E}$ be an edge of a Lipschitz domain Ω_i and define a finite element function $\theta_{\mathcal{E}}$ which equals 1 at all nodes of $\mathcal{E}$, vanishes at all other nodes of $\partial\Omega_i$, and is discrete harmonic. Then,*

$$|\theta_{\mathcal{E}}|^2_{H^1(\Omega_i)} \leq CH_i.$$

Proof. We only have to consider the function which equals 1 at the nodes of $\mathcal{E}$ and vanishes at all other nodes of the closure of Ω_i and use the fact that for a Lipschitz subregion, there are at most CH_i/h_i nodes on $\mathcal{E}$. Each nodal basis function has a H^1-norm squared of order h_i. The discrete harmonic extension of the related boundary values will provide a function with even smaller energy. ∎

By using these two lemmas, we can conclude that for Option 1

$$E_i(\phi_{ic}) \leq C(1 + \log(H_i/h_i))H_i\rho_i.$$

When we turn to estimates of the coefficients multiplying the coarse basis functions in our interpolation formula, we will need a bound on the average over subdomain edges of finite element functions. We obtain this bound by using the Cauchy-Schwarz inequality and the following lemma, which generalizes [16, Lemma 3.1] to the case of edges of Lipschitz subdomains. We note that this result can be considered a discrete Sobolev inequality.

LEMMA 3. *Let u be any continuous, piecewise linear function on a Lipschitz subdomain Ω_i of diameter H_i partitioned into a quasi-uniform mesh with a minimal mesh size h_i. Then for any edge $\mathcal{E}$ of the subdomain*

$$\|u\|^2_{L^2(\mathcal{E})} \leq C(\Omega_i)(1+\log(H_i/h_i))\|u\|^2_{H^1(\Omega_i)}$$

and

$$\|u-\bar{u}_{\mathcal{E}}\|^2_{L^2(\mathcal{E})} \leq C(\Omega_i)(1+\log(H_i/h_i))|u|^2_{H^1(\Omega_i)}.$$

Here $\bar{u}_{\mathcal{E}}$ is the average of u over the edge $\mathcal{E}$ and $C(\Omega_i)$ a constant independent of the mesh size.

Proof. We follow the proof of [16, Lemma 3.1] closely, which in turn derives its main idea from the proof of a well-known finite element Sobolev inequality in two dimensions as provided in [3, Lemma 4.15]. In our previous proof for tetrahedral subdomains, we considered the centroids c_K of any element in Ω_i with at least one vertex of the edge $\mathcal{E}$ and constructed sets of planes through these centroids each parallel to one of two faces of the tetrahedron; each intersection of any of these planes with the tetrahedron also has an area on the order of H_i^2. A similar construction is clearly possible for any Lipschitz subdomain; we recall that the boundary of a Lipschitz domain can be covered by a finite number of patches and that for each such patch we can introduce a local coordinate system with one coordinate playing the role of an average normal; the patch can then be represented by a Lipschitz function of the remaining variables. In addition, this local part of the subdomain boundary can be shifted a distance proportional to the diameter of the subdomain in the direction of this normal while staying inside the subdomain. We also note that a local argument in our earlier proof, borrowed from Brenner–Scott, provides an estimate of the value of u at an edge node in terms of that for the value at the centroid of the related element is still valid. ∎

Let $\bar{u}_i$, $\bar{u}_{\mathcal{F}}$, $\bar{u}_{\mathcal{E}}$ denote the mean of a finite element function u over the subdomain Ω_i, a subdomain face $\mathcal{F}$, and a subdomain edge $\mathcal{E}$, respectively. For a face $\mathcal{F}$ of Ω_i, it follows from a trace theorem, which is valid for all Lipschitz domains, that

$$\|u\|^2_{L^2(\mathcal{F})} \leq CH_i(\|\nabla u\|^2_{L^2(\Omega_i)} + H_i^{-2}\|u\|^2_{L^2(\Omega_i)}), \tag{7}$$

see, e.g., [29, Subsection 1.1.3], and from the Cauchy–Schwarz and Poincaré inequalities that

$$\rho_i H_i|\bar{u}_{\mathcal{F}} - \bar{u}_i|^2 \leq CE_i(u^{(i)}). \tag{8}$$

Similarly, for an edge $\mathcal{E}$ of Ω_i, we find by using Lemma 3 and the Cauchy–Schwarz and Poincaré inequalities that

$$\rho_i H_i|\bar{u}_{\mathcal{E}} - \bar{u}_i|^2 \leq C(1+\log(H_i/h_i))E_i(u^{(i)}). \tag{9}$$

We will now consider two different assumptions on the coefficient, ρ, of the scalar elliptic problems. We will use the same assumptions for μ, one of the Lamé parameters, when we consider linear elasticity problems.

ASSUMPTION 1. *Let c be any coarse node of Ω_i and $\mathcal{S}_c$ be the index set of all subdomains containing c on their boundaries. Select $j_c \in \mathcal{S}_c$ such that $\rho_{j_c} \geq \rho_j$ for all $j \in \mathcal{S}_c$. Assume that there exists a constant C and for any $i \in \mathcal{S}_c$ a sequence $\{i = j_c^0, j_c^1, ..., j_c^p = j_c\}$, all in $\mathcal{S}_c$, such that $\rho_i \leq C\rho_{j_c^\ell}$ and that $\Omega_{j_c^{\ell-1}}$ and $\Omega_{j_c^\ell}$ have a subdomain face $\mathcal{F}_{j_c^{\ell-1},j_c^\ell}$ in common for all $\ell = 1, \ldots, p$ and $i = 1, \ldots, N$. In the case that $c \in \partial\Omega$, we also assume that $\partial\Omega_{j_c} \cap \partial\Omega$ contains at least one subdomain face.*

In other words, Assumption 1 means that there is a face connected path between Ω_i and Ω_{j_c} such that the diffusion coefficient ρ_i is no greater than a constant times the diffusion coefficient of any subdomain along the path. This assumption appears to be essentially the same as the quasi-monotonicity assumption of [17]. If Assumption 1 is satisfied, we will say that we have *monotone face-connected paths.*

ASSUMPTION 2. *Using the same notation as in Assumption 1, assume that there exists a sequence $\{i = j_c^0, j_c^1, ..., j_c^p = j_c\}$, all in $\mathcal{S}_c$, such that $\rho_i \leq C\rho_{j_c^\ell}$ and $\Omega_{j_c^{\ell-1}}$ and $\Omega_{j_c^\ell}$ have at least a subdomain edge in common for all $\ell = 1, \ldots, p$ and $i = 1, \ldots, N$. In the case that $c \in \partial\Omega_i$ also assume that $\partial\Omega_{j_c} \cap \partial\Omega$ contains at least one subdomain edge.*

We note that Assumption 2 is weaker than Assumption 1 since we have more options of continuing at every step in the construction of a path. If Assumption 2 is satisfied, we will say that we have *monotone edge-connected paths.*

Our analysis can closely follow the theory as developed in [36, Section 2.3]; the main effort is directed to obtaining a good bound of the energy of the coarse component, commonly denoted by u_0, in the decomposition of an arbitrary element of our finite element space.

Since the sum of the coarse basis functions for any subdomain Ω_i equals 1, prior to the imposition of essential boundary conditions, we find that

$$E_i(\sum_{c\in\mathcal{M}_{ic}} \bar{u}_i\phi_{ic}) = 0. \tag{10}$$

We first consider the case when the boundary of the subdomain Ω_i does not intersect $\partial\Omega$. The restriction of the coarse component to Ω_i is then chosen as

$$u_0^{(i)} = \sum_{c\in\mathcal{M}_{ic}} \bar{u}_{j_c}\phi_{ic}, \tag{11}$$

where $\bar{u}_{j_c}$ is the average of u over the subdomain Ω_{j_c}, with j_c chosen as in Assumption 1 and $\mathcal{M}_{ic}$ the set of coarse nodes for Ω_i. We note that the values of the coefficients $\bar{u}_{j_c}$ often will be imported from different neighboring subdomains.

We will next establish bounds for $E_i(u_0^{(i)})$. By using a face connected path as in Assumption 1, and assuming Option 2, we start with

$$\bar{u}_i - \bar{u}_{j_c} = (\bar{u}_i - \bar{u}_{\mathcal{F}_{j_c^0 j_c^1}}) + \sum_{\ell=1}^{p-1}(\bar{u}_{\mathcal{F}_{j_c^{\ell-1} j_c^\ell}} - \bar{u}_{\mathcal{F}_{j_c^\ell j_c^{\ell+1}}}) + (\bar{u}_{\mathcal{F}_{j_c^{p-1} j_c^p}} - \bar{u}_{j_c}), \tag{12}$$

where $\mathcal{F}_{j_c^{\ell-1} j_c^\ell}$ denotes the face common to $\Omega_{j_c^{\ell-1}}$ and $\Omega_{j_c^\ell}$. Rewriting a term in the sum as

$$\bar{u}_{\mathcal{F}_{j_c^{\ell-1} j_c^\ell}} - \bar{u}_{\mathcal{F}_{j_c^\ell j_c^{\ell+1}}} = (\bar{u}_{\mathcal{F}_{j_c^{\ell-1} j_c^\ell}} - \bar{u}_{j_c^\ell}) - (\bar{u}_{\mathcal{F}_{j_c^\ell j_c^{\ell+1}}} - \bar{u}_{j_c^\ell}), \tag{13}$$

and by using Assumption 1 and (8), we find that

$$\rho_i H_i |\bar{u}_i - \bar{u}_{j_c}|^2 \leq C \sum_{j \in \mathcal{S}_c} E_j(u^{(j)}).$$

It then follows from (6) that

$$E_i((\bar{u}_i - \bar{u}_{j_c})\phi_{ic}) \leq C \sum_{j \in \mathcal{S}_c} E_j(u^{(j)}).$$

If Ω_i is an interior subdomain, we then obtain, using (10),

$$E_i(u_0^{(i)}) \leq C \sum_{j \in \mathcal{M}_{is}} E_j(u^{(j)}),$$

where $\mathcal{M}_{is}$ is the index set of all subdomains adjacent to Ω_i and Ω_i itself.

In case $\partial\Omega_i$ intersects $\partial\Omega$, we make a modification of the coarse interpolant (11) by replacing the coefficients $\bar{u}_{j_c}$ associated with coarse nodes on $\partial\Omega$ by the average over the subdomain face or subdomain edge of Ω_{j_c} which exists according to the assumptions. We easily obtain the same inequalities as before. We note that the terms corresponding to coarse nodes on $\partial\Omega$ will simply vanish since the average over these special subdomain faces or edges equals zero because of the zero Dirichlet condition for the elliptic problem. This shows that the coarse interpolant belongs to the correct finite element space.

Adding the contributions from all subdomains and noting that $|\mathcal{M}_{is}| \leq C$, we see that the energy of our coarse interpolant is uniformly bounded by the energy of u under Assumption 1,

$$\sum_{i=1}^{N} E_i(u_0^{(i)}) \leq C \sum_{i=1}^{N} E_i(u^{(i)}). \tag{14}$$

We can now replace the face averages in (12) and (13) by edge averages as in Assumption 2. By using (9) instead of (8) in the previous development, we find under the less restrictive Assumption 2 that

$$\sum_{i=1}^{N} E_i(u_0^{(i)}) \leq C(1 + \log(H/h)) \sum_{i=1}^{N} E_i(u^{(i)}), \tag{15}$$

where $H/h := \max_i(H_i/h_i)$.

If the coarse basis functions originate from (1) rather than (2,5), then it follows from elementary estimates and Lemma 3 that $1 + \log(H_i/h_i)$ will appear as an additional factor on the right-hand-side of (6). Thus, this additional factor will also be present in (14) and (15).

With the estimates for our coarse interpolants in hand, we can now perform a local analysis for an overlapping additive Schwarz algorithm using basically the same approach as in [10] or [13]. This involves a partition of unity $\{\vartheta_i\}_{i=1}^N$ with $0 \leq \vartheta_i \leq 1$, $|\nabla\vartheta_i| \leq C/\delta_i$, and with ϑ_i supported in the closure of the overlapping subdomain Ω_i'. Here, δ_i is the thickness of the part of Ω_i' which is common with its neighbors. Given an estimate of the form

$$\sum_{i=1}^{N} E_i(u_0^{(i)}) \leq C\Theta(H/h) \sum_{i=1}^{N} E_i(u^{(i)}),$$

the resulting condition number estimate for the preconditioned operator is given by

$$\kappa(M^{-1}A) \leq C\Theta(H/h)(1+H/\delta), \tag{16}$$

where $H/\delta := \max_i H_i/\delta_i$. Comparing (16) with (14) and (15), we see that $\Theta(H/h)$ is 1, $1+\log(H/h)$, or even $(1+\log(H/h))^2$ under Assumption 1 and Option 2, Assumption 1 and Option 1 or Assumption 2 and Option 2, and Assumption 2 and Option 1, respectively.

We note that these coarse spaces could alternatively be combined with local spaces previously developed for iterative substructuring algorithms such as those of [18]; see also [36, Chapter 5].

5. Compressible Linear Elasticity and Korn's Second Inequality. We now turn to the equations of linear elasticity. Let $\Omega \subset \mathbb{R}^3$ be a domain with a Lipschitz boundary, and let $\partial\Omega_D$, be a nonempty subset of its boundary $\partial\Omega$, and introduce the Sobolev space $\mathbf{V} := \{\mathbf{v} \in \mathbf{H}^1(\Omega) : \mathbf{v}|_{\partial\Omega_D} = 0\}$. Here, $\mathbf{H}^1(\Omega) := H^1(\Omega)^3$. The linear elasticity problem consists in finding the displacement $\mathbf{u} \in \mathbf{V}$ of the domain Ω, fixed along $\partial\Omega_D$ and with a surface force of density $\mathbf{g}$, along $\partial\Omega_N := \partial\Omega \setminus \partial\Omega_D$, and with a body force $\mathbf{f}$:

$$a(\mathbf{u},\mathbf{v}) := 2\int_\Omega \mu\ \epsilon(\mathbf{u}) : \epsilon(\mathbf{v})\ dx + \int_\Omega \lambda\ \text{div}\ \boldsymbol{u}\ \text{div}\ \boldsymbol{v}\ dx\ =\ \langle \mathbf{F},\mathbf{v}\rangle \quad \forall \mathbf{v} \in \mathbf{V}.$$

Here $\lambda(x)$ and $\mu(x)$ are the Lamé parameters, $\epsilon_{ij}(\mathbf{u}) = \frac{1}{2}(\frac{\partial u_i}{\partial x_j} + \frac{\partial u_j}{\partial x_i})$ is the linearized strain tensor, and two inner products are defined by

$$\epsilon(\mathbf{u}) : \epsilon(\mathbf{v}) := \sum_{i=1}^{3}\sum_{j=1}^{3} \epsilon_{ij}(\mathbf{u})\epsilon_{ij}(\mathbf{v}),\ \langle \mathbf{F},\mathbf{v}\rangle\ :=\ \int_\Omega \sum_{i=1}^{3} f_i v_i\ dx + \int_{\partial\Omega_N} \sum_{i=1}^{3} g_i v_i\ ds. \tag{17}$$

The Lamé parameters can be expressed in terms of the Poisson ratio ν and Young's modulus E:

$$\mu = \frac{E}{2(1+\nu)}, \qquad \lambda = \frac{E\nu}{(1+\nu)(1-2\nu)} = \frac{2\nu}{1-2\nu}\mu.$$

In our proofs, we will always assume that the Lamé parameters are constant in each subdomain and denote their values in Ω_i by μ_i and λ_i, respectively. The parameter μ_i will play a role similar to that of ρ_i in the analysis of the scalar case. We will also assume that we have a zero Dirichlet condition on all of $\partial\Omega$ just as for the scalar elliptic problem.

We note that the factor $\frac{2\nu}{1-2\nu}$ is bounded for the compressible case for which $\nu < 1/2$. We note that we then have the upper bound

$$a_i(\mathbf{u},\mathbf{u}) \leq \frac{2(1+\nu_i)}{1-2\nu_i}\mu_i |\mathbf{u}|^2_{\mathbf{H}^1(\Omega_i)},$$

where $a_i(\mathbf{u},\mathbf{v})$ is the contribution of Ω_i to $a(\mathbf{u},\mathbf{v})$. The ellipticity of this problem is established by using Korn's first inequality cf., e.g., [31].

In this study, we need to use Korn's second inequality:

LEMMA 4 (Korn's second inequality). *Let $\Omega \subset \mathbb{R}^3$ be a Lipschitz domain of diameter H. Then, there exists a positive constant $C = C(\Omega)$, such that*

$$|\mathbf{u}|^2_{\mathbf{H}^1(\Omega)} + \frac{1}{H^2}\|\mathbf{u}\|^2_{\mathbf{L}^2(\Omega)} \leq C(\Omega)\,(\int_\Omega \varepsilon(\mathbf{u}) : \varepsilon(\mathbf{u})dx + \frac{1}{H^2}\|\mathbf{u}\|^2_{\mathbf{L}^2(\Omega)}) \quad \forall \mathbf{u} \in \mathbf{H}^1(\Omega).$$

There are several proofs; see, e.g., [31].

When analyzing linear elasticity, we need a replacement of Poincaré's inequality:

LEMMA 5. *Let Ω be a Lipschitz domain. There then exist a constant $C(\Omega)$ such that*

$$\inf_{\mathbf{r}\in\mathcal{RB}} \|\mathbf{u}-\mathbf{r}\|^2_{\mathbf{H}^1(\Omega)} \leq C(\Omega)\int_\Omega \varepsilon(\mathbf{u}):\varepsilon(\mathbf{u})dx,\ \ \forall \mathbf{u}\in\mathbf{H}^1(\Omega).$$

Here $\mathcal{RB}$ is the space of rigid body modes.

A proof can be found in [30, Section 6.3]

We note that this result has been used for similar purposes in [11, Lemma 5.2]. A number of variants of Korn's inequalities is provided in [27, Section 6].

6. Analysis of Linear Elasticity. Turning to the analysis of the linear elasticity case, we will always assume that Assumption 1 holds.

Associated with each coarse node c are six degrees of freedom and six coarse basis functions directly associated with the six rigid body modes of formulas (3) and (4). In our proof, we will rely on the fact that the sum of the basis functions of the coarse nodes of any subdomain will give us the basis functions for the space of rigid body modes. This follows from the fact that we have a partition of unity defined by the p_{nc}; see (1) or (2) and (5).

Estimates of the energy of the individual basis functions do not pose any challenges in addition to those of Section 4.

We need to decide how to replace the averages over the subdomains and the subdomain faces that play an important part in the proof in the scalar case. They are replaced by using two mappings into $\mathcal{RB}$, the space of rigid body modes. We first introduce, for $k=1,\ldots 6$, the functionals

$$g_k^{(i)V}(\mathbf{u}) := \frac{\int_{\Omega_i}\mathbf{u}\cdot\mathbf{r}_k dx}{\int_{\Omega_i}\mathbf{r}_k\cdot\mathbf{r}_k dx} \quad \textit{and} \quad g_k^{(i)\mathcal{F}}(\mathbf{u}) := \frac{\int_{\mathcal{F}}\mathbf{u}\cdot\mathbf{r}_k dA}{\int_{\mathcal{F}}\mathbf{r}_k\cdot\mathbf{r}_k dA},$$

where $\mathcal{F}$ is a face common to two subdomains Ω_i and Ω_j.

To simplify or estimates, we replace the three rigid body modes $\boldsymbol{r}_4, \boldsymbol{r}_5$, and $\boldsymbol{r}_6$ by dividing these functions by H_i. This results in six functions spanning the space of rigid body modes which all have an $\mathbf{L}^2(\Omega_i)-$norm on the order of $H_i^{3/2}$ and an $\mathbf{L}^2(\mathcal{F})-$norm on the order of H_i.

We next create two dual bases by using linear combinations

$$f_k^{(i)V}(\mathbf{u}) := \sum_{m=1}^{6}\beta_{km}g_m^{(i)V}(\mathbf{u}) \quad \textit{and} \quad f_k^{(i)\mathcal{F}}(\mathbf{u}) := \sum_{m=1}^{6}\gamma_{km}g_m^{(i)\mathcal{F}}(\mathbf{u})$$

such that

$$f_k^{(i)V}(\boldsymbol{r}_\ell) = \delta_{\ell,k} \quad \textit{and} \quad f_k^{(i)\mathcal{F}}(\boldsymbol{r}_\ell) = \delta_{\ell,k}.$$

Using that the rigid body modes are linearly independent, we find that the coefficients β_{km} and γ_{km} are all of order 1. It then easily follows that

$$|f_k^{(i)V}(\boldsymbol{u})| \leq C\|\boldsymbol{u}\|_{\mathbf{H}^1(\Omega_i)}/H_i$$

and, by using the trace theorem (7), that

$$|f_k^{(i)\mathcal{F}}(\boldsymbol{u})| \leq C\|\boldsymbol{u}\|_{L^2(\mathcal{F})}/H_i^2 \leq C\|\boldsymbol{u}\|_{\mathbf{H}^1(\Omega_i)}/H_i.$$

We can then replace $\bar{u}_{\mathcal{F}}$ and $\bar{u}_i$ by

$$\sum_{k=1}^{6} f_k^{(i)\mathcal{F}}(\mathbf{u})\mathbf{r}_k \quad \textit{and} \quad \sum_{k=1}^{6} f_k^{(i)V}(\mathbf{u})\mathbf{r}_k \tag{18}$$

and then follow the proof for the scalar case. We note that the linear functions of (18) both reproduce any rigid body mode. Thus, we obtain

$$\sum_{k=1}^{6} f_k^{(i)\mathcal{F}}(\mathbf{u})\mathbf{r}_k - \sum_{k=1}^{6} f_k^{(i)V}(\mathbf{u})\mathbf{r}_k = \sum_{k=1}^{6} f_k^{(i)\mathcal{F}}(\mathbf{u}-\mathbf{r})\mathbf{r}_k - \sum_{k=1}^{6} f_k^{(i)V}(\mathbf{u}-\mathbf{r})\mathbf{r}_k.$$

Each term of the sums can be bounded by $\|\mathbf{u}-\mathbf{r}\|_{\mathbf{H}^1}/H_i$. This allows us to use Lemma 5 and complete the estimate just as for the scalar elliptic problem. Since we use Assumption 1, we will have one $(1+\log(H/h))$ factor if we use Option 1.

7. Numerical Examples. Numerical results are presented in this section to confirm the theory and to demonstrate the computational advantages of the small coarse spaces. The number of conjugate gradient iterations (iter) to achieve a relative residual tolerance of 10^{-8} for the solution of $Ax = b$ and associated estimates of condition numbers (cond) for the preconditioned operator are reported in the following tables. With the exception of the almost incompressible elasticity example, the subdomains are discretized using lowest order hexahedral, Q_1, nodal elements. Random right-hand-side vectors b are used for all the examples, and table headings of *Option 1* and *Option 2* refer to the use of formulas in (1) and (2,5), respectively.

The first three examples are for a unit cube domain with homogeneous essential boundary conditions on one of its faces. In the first example, the domain is decomposed into smaller cubic subdomains with the number of elements in each of the three coordinate directions denoted by H/h. In addition to the coarse spaces of this study, we also consider a larger one which uses vertex, edge, and face equivalence classes as in [11]. We refer to this coarse space as the *full one*.

The results in Table 1 confirm that condition numbers are bounded independently of the number of subdomains for all three coarse spaces. Notice also that the dimensions of the small coarse spaces are significantly smaller than those of the full coarse space. Further, we observe only a modest increase in iterations and condition numbers when using the small coarse spaces.

The second example is identical to the first except that the subdomains are now obtained using a mesh partitioner based on METIS, [23]. We note in some cases that METIS may generate a relatively small number of disconnected subdomains. In such cases, we treat each of the disconnected components as a separate subdomain. The results in Table 2 also confirm scalability with respect to the number of subdomains. The smaller coarse spaces are significantly smaller than the full ones, but not to the same extent as for the regular decompositions in Table 1. Again, the numbers of iterations and condition numbers are only slightly larger when using the small coarse spaces.

The third example investigates the dependence of condition numbers on the ratio H/h for a unit cube domain decomposed into 125 smaller cubic subdomains while holding the overlap parameter $H/\delta = 4$ fixed. Condition numbers from the top half of Table 3 are plotted versus $\log(H/h)$ in Figure 1. Notice that the growth with respect to $\log(H/h)$ appears to be consistent with the theory, and the line segment slope for Option 2 is smaller than those for the other two coarse spaces.

TABLE 1

Results for a unit cube decomposed into smaller cubic subdomains with $H/h = 4$ and overlap $H/\delta = 4$. The material properties are constant with $\rho = 1$ for scalar problems and $E = 1$, $\nu = 0.3$ for elasticity problems. Coarse space dimensions are denoted by N_c.

	full coarse space			small coarse spaces				
					Option 1		Option 2	
N	N_c	iter	cond	N_c	iter	cond	iter	cond
scalar problem results								
64	279	29	15.1	27	36	21.8	34	20.4
216	1115	30	15.7	125	41	23.5	38	21.4
512	2863	31	16.0	343	42	24.4	38	21.9
1000	5859	32	16.2	729	43	25.0	39	22.2
1728	10439	32	16.3	1331	44	25.3	40	22.3
elasticity problem results								
64	1485	33	15.0	162	42	20.7	40	18.6
216	5865	36	15.9	750	45	21.3	40	18.6
512	14973	37	16.4	2058	46	21.7	41	18.7
1000	30537	38	16.6	4374	46	21.8	42	18.6
1728	54285	38	16.7	7986	47	21.8	42	18.6

TABLE 2

Results for a unit cube decomposed into subdomains using a mesh partitioner. Material properties, numbers of elements for the meshes, and the overlap parameter are the same as those for Table 1. Coarse space dimensions are denoted by N_c.

	full coarse space			small coarse spaces				
					Option 1		Option 2	
N	N_c	iter	cond	N_c	iter	cond	iter	cond
scalar problem results								
64	399	36	16.2	66	43	19.7	41	18.3
216	2500	39	18.3	590	42	20.5	40	18.0
512	5844	39	16.3	1450	44	19.5	43	17.9
1005	13151	41	18.5	3363	45	19.8	43	17.8
1729	24410	41	17.7	6426	45	19.9	43	18.5
elasticity problem results								
64	1961	39	16.1	396	46	20.2	44	18.9
216	11064	41	17.3	3539	44	18.6	40	16.0
512	25869	41	15.8	8700	45	18.7	43	17.1
1005	56907	43	16.9	20178	45	18.2	44	17.2
1729	104172	43	17.2	38553	46	18.3	43	17.4

TABLE 3

Results for a unit cube decomposed into 125 smaller cubic subdomains with overlap $H/\delta = 4$. The material properties are constant with $\rho = 1$ for scalar problems and $E = 1$, $\nu = 0.3$ for elasticity problems.

	full coarse space		small coarse spaces			
			Option 1		Option 2	
H/h	iter	cond	iter	cond	iter	cond
scalar problem results						
3	27	12.3	34	17.5	33	16.5
6	35	18.2	38	24.5	35	21.1
9	38	21.9	41	28.8	36	23.4
12	39	24.5	42	31.8	37	24.9
elasticity problem results						
3	32	13.0	39	17.1	36	15.4
6	40	16.9	45	22.0	40	18.2
9	43	19.4	48	25.0	42	19.7
12	45	21.2	51	27.1	44	20.7

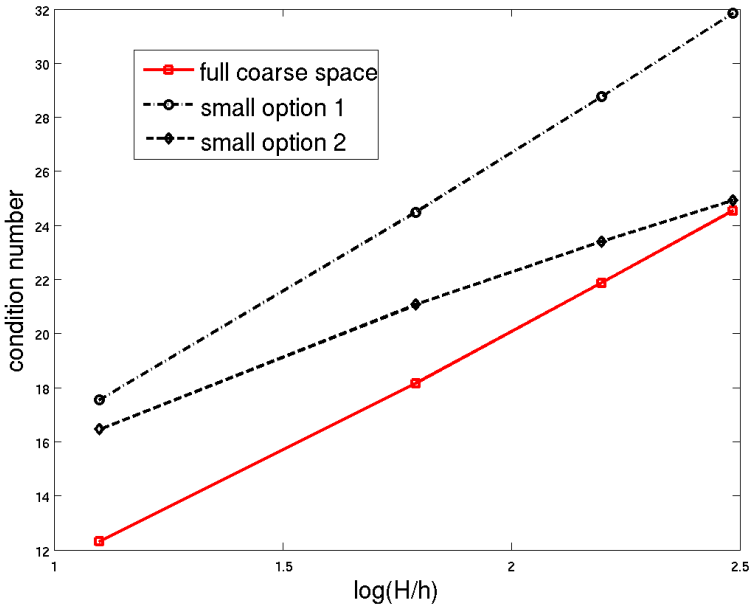

FIG. 1. *Plot of condition numbers in top half of Table 3 versus* $\log(H/h)$.

TABLE 4

Results for a unit cube decomposed into 64 smaller cubic subdomains with $H/h = 12$. *The material properties are constant with* $\rho = 1$ *for scalar problems and* $E = 1$, $\nu = 0.3$ *for elasticity problems.*

	full coarse space		small coarse spaces			
			Option 1		Option 2	
H/δ	iter	cond	iter	cond	iter	cond
scalar problem results						
2	35	20.9	36	27.0	34	19.2
3	38	23.4	39	30.6	35	23.9
4	41	24.9	43	33.3	38	27.6
6	43	27.4	47	38.6	43	34.3
12	47	37.1	60	55.8	56	53.6
elasticity problem results						
2	38	17.2	44	23.2	39	16.7
3	42	19.9	49	26.2	42	20.3
4	44	21.3	52	28.8	46	23.2
6	47	23.5	56	33.6	51	28.6
12	51	34.8	69	51.9	64	48.6

The fourth example deals with the dependence of condition numbers on the ratio H/δ for a unit cube domain decomposed into 64 smaller cubic subdomains with $H/h = 12$. The results in the top half of Table 4 for condition numbers of the two smaller coarse spaces are shown in Figure 2. The near linear growth of condition numbers with respect to H/δ is consistent with the theory.

The next three examples investigate the dependence of condition numbers on H/h for fixed $H/\delta = 4$ and different arrangements of material properties. The scarlet regions in Figure 3 have $\rho = 10^4$, $E = 10^4$ and $\nu = 0.3$, while the gray regions have

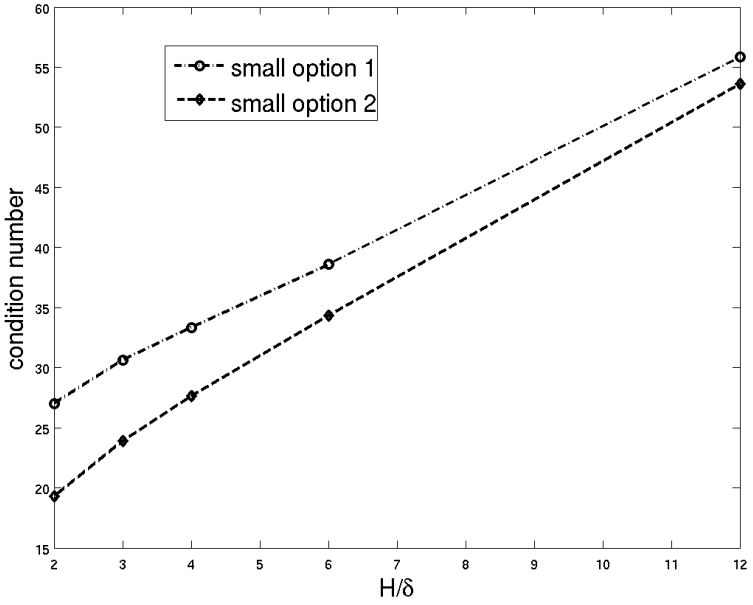

FIG. 2. *Plot of condition numbers in top half of Table 4 versus H/δ.*

$\rho = 1$, $E = 1$ and $\nu = 0.3$.

The results in Table 5 correspond to upper left Figure 3 where there are always monotone face-connected paths between the subdomains. Similarly, the results in Table 6 correspond to upper right Figure 3 where some monotone paths between subdomains are only edge-connected. As is evident in the table, this example demonstrates the importance of having monotone face-connected paths when using the small coarse spaces for elasticity problems. Finally, the results in Table 7 correspond to the bottom two figures in Figure 3 where there exist neither monotone face-connected nor edge-connected paths between the subdomains. Plotting condition numbers from the top halves of these three tables versus $\log(H/h)$ in Figure 4 for the small coarse spaces reveals that condition numbers for cases with face and edge connected paths appear to have no greater than a linear dependence on $\log(H/h)$. Remarkably, results for when neither face nor edge connected paths are present have the smallest condition numbers. This case is not covered by our theory, and the asymptotic behavior for larger values of $\log(H/h)$ is less clear than for the other two.

The next example deals with an almost incompressible elasticity problem discretized using 27-node quadratic, hexahedral, Q_2 elements. Discontinuous linear, P_1 pressures are statically condensed in this inf-sup stable mixed formulation of elasticity to obtain a fully displacement-based element as described in [11]. Results are presented in Table 8 for a unit cube mesh of 16^3 elements with essential boundary conditions applied over the entire boundary and decomposed into either 64 cubic subdomains or 64 subdomains from a mesh partitioner. Although the results in Table 8 are less sensitive to Poisson's ratio ν for the full coarse space, the performance of the smaller coarse spaces remains satisfactory. As might be expected, the addition of a single normal degree of freedom to each subdomain face for the smaller coarse spaces

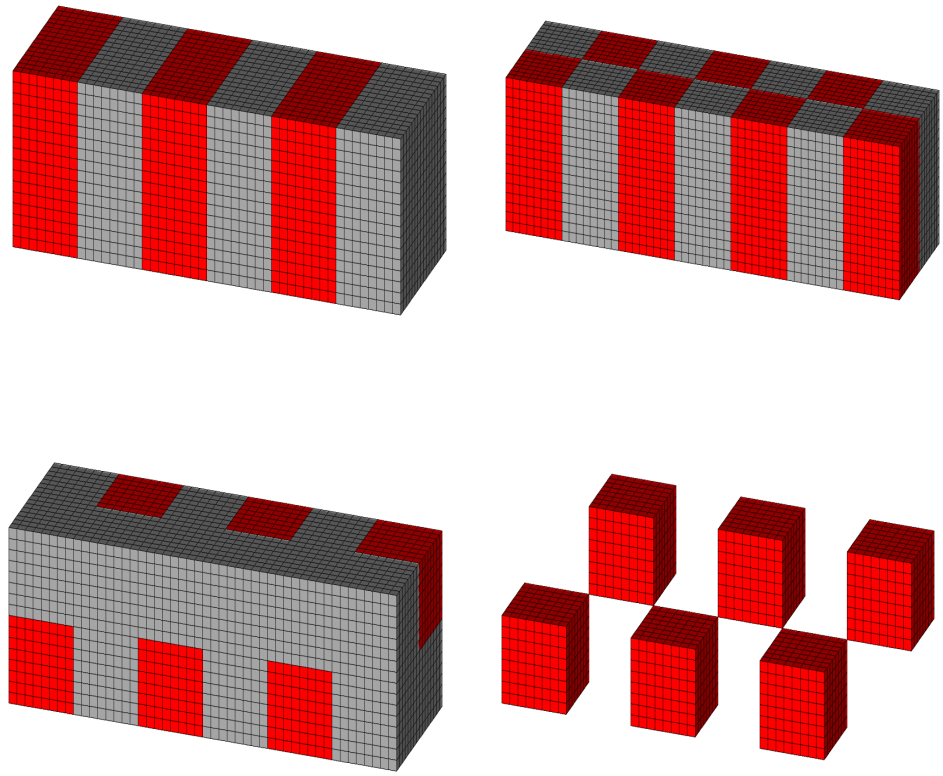

FIG. 3. *Meshes with 2 cubic subdomains in each direction orthogonal to the domain axis for* $H/h = 8$. *Scarlet regions have* $\rho = \sigma$, $E = \sigma$, $\nu = 0.3$, *while the gray ones have* $\rho = 1$, $E = 1$, *and* $\nu = 0.3$. *The upper left and right figures have monotone face-connected and edge-connected paths, respectively, while the bottom left one has neither. The lower right figure shows the lower left figure with gray regions removed.*

leads to improved results as ν approaches $1/2$ as shown in the final four columns of Table 8. We have yet to develop an accompanying theory, but the benefits of adding the normal decree of freedom has been observed previously for a different coarse space [12]. We note for regular arrangements of cubic subdomains that the coarse space dimension increases from about $6N$ to $9N$ with the addition of a face normal degree of freedom since each faces is shared by two subdomains.

The final example concerns the use of preconditioners with symmetric multiplicative corrections at the subdomain and coarse levels as opposed to the additive Schwarz form considered thus far; see the discussion of such methods on [36, Page 38]. Our interest in these preconditioners is motivated by the desire for inexact yet high quality subdomain solvers for compute platforms with many cores per node. The idea here is to replace a direct solver for a subdomain on a compute node with an approximate one requiring much less memory. Application of such preconditioners requires one coarse solve and two local solves for each subdomain per iteration, but can result in

TABLE 5

Results for monotone face-connected paths between subdomains (see Figure 3 upper left) with overlap $H/\delta = 4$.

	full coarse space		small coarse spaces			
			Option 1		Option 2	
H/h	iter	cond	iter	cond	iter	cond
scalar problem results						
3	26	11.4	28	21.9	27	21.9
6	36	16.0	33	31.5	30	31.2
9	36	18.9	34	37.3	31	36.8
12	37	20.9	35	41.4	31	40.7
elasticity problem results						
3	32	11.8	43	34.0	42	33.9
6	41	14.5	52	52.7	46	52.2
9	44	16.3	58	64.2	49	63.4
12	46	17.6	61	72.5	49	71.4

TABLE 6

*Results for monotone edge-connected paths between subdomains (see Figure 3 upper right) with overlap $H/\delta = 4$. The symbol * means convergence was not achieved within 100 iterations.*

	full coarse space		small coarse spaces			
			Option 1		Option 2	
H/h	iter	cond	iter	cond	iter	cond
scalar problem results						
3	26	10.8	40	49.3	40	45.2
6	34	13.7	44	76.1	44	59.1
9	37	15.4	46	95.5	45	67.4
12	38	16.6	48	111	46	73.3
elasticity problem results						
3	39	15.0	100	1.46×10^4	*	1.33×10^4
6	50	21.7	100	1.93×10^4	*	1.42×10^4
9	56	25.9	100	2.25×10^4	*	1.48×10^4
12	59	29.0	100	2.48×10^4	*	1.52×10^4

significant improvements. For example, the numbers of iterations in the first row of Table 1 are reduced from (29, 36, 34) to (8, 10, 9). Likewise, condition numbers are reduced from (15.1, 21.8, 20.4) to (1.4, 1.8, 1.7); these results were obtained using exact coarse and local solvers. We expect the use of inexact subdomain solvers to play a more prominent role on future computing platforms.

As a final note, the small coarse spaces of this study can also be used successfully with iterative substructuring preconditioners like the one in [12] which also uses overlapping Schwarz concepts. Due to page limitations, we are unable to present any numerical results, but a small coarse space based on Option 1 has been used to solve a wide variety of problems using the Sierra structural dynamics module [34]. There, the iterative solver is called GDSW (Generalized Dryja Smith Widlund) since it uses a coarse space built on the pioneering work in [18].

TABLE 7

Results for bottom two figures in Figure 3) with overlap $H/\delta = 4$. Here, there may not exist either a monotone face-connected or edge-connected path between subdomains.

	full coarse space		small coarse spaces			
			Option 1		Option 2	
H/h	iter	cond	iter	cond	iter	cond
scalar problem results						
3	25	11.1	33	19.5	31	19.502
6	33	14.9	36	23.9	34	20.5
9	35	17.2	36	27.3	35	22.0
12	35	18.9	37	29.8	36	22.9

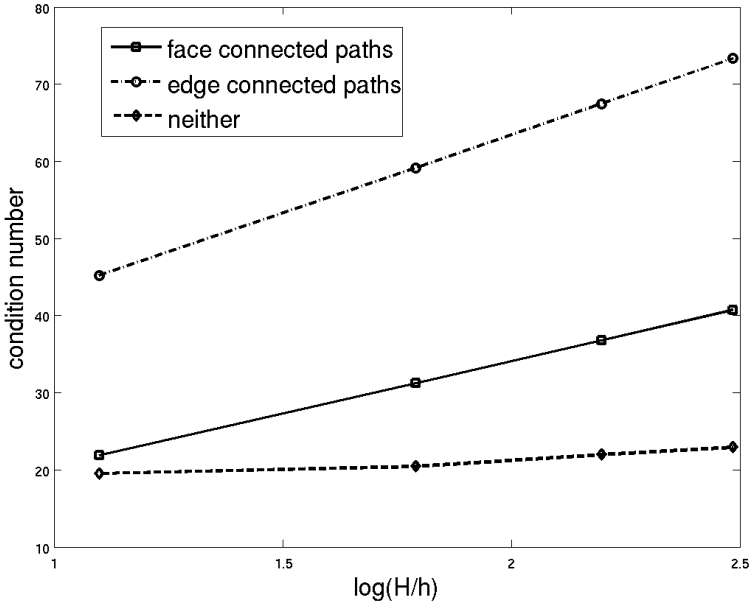

FIG. 4. *Plot of condition numbers in top halves of Tables 5-7 for small coarse space Option 1.*

REFERENCES

[1] Report on the Workshop on Extreme-Scale Solvers: Transition to Future Architectures. Technical Report, U.S. Department of Energy Office of Advanced Scientific Computing Research, 2012.

[2] Bramble, J.H. and Xu, J.: Some estimates for a weighted L^2 projection. Math. Comp., **56** (194), 463–476 (1991).

[3] Brenner S.C. and Scott, R.: The Mathematical Theory of Finite Element Methods, third edition. *Springer*, 2008.

[4] Cai, M., Pavarino, L.F., and Widlund, O.B.: Overlapping Schwarz methods with a standard coarse space for almost incompressible linear elasticity. SIAM J. Sci. Comput. **37**(2), A811–A830 (2015).

[5] Cai, M. and Pavarino, L.F.: Hybrid and Multiplicative Overlapping Schwarz Algorithms with Standard Coarse Spaces for Mixed Linear Elasticity and Stokes Problems, Comm. Comput. Phys. **20** (4), 989–1015 (2016).

[6] Calvo, J.G.: A two-level overlapping Schwarz method for H(curl) in two dimensions with irregular subdomains. Electron. Trans. Numer. Anal. **44**, 497–521 (2015).

[7] Calvo, J.G.: A BDDC algorithm with deluxe scaling for H(curl) in two dimensions with irregular

TABLE 8

Results for almost incompressible elasticity problem. The elastic modulus is $E = 1$ and Poisson's ratio increases from 0.3 to near the incompressible limit of 1/2. Results in the final four columns in the table were obtained by including a normal degree of freedom (dof) for each subdomain face in the coarse space.

	full coarse space		small coarse spaces							
			no face normal dof				added face normal dof			
			Option 1		Option 2		Option 1		Option 2	
H/h	iter	cond	iter	cond	iter	cond	iter	cond	iter	cond
decompositions into cubic subdomains										
0.3	31	12.8	33	15.7	32	14.2	33	14.7	31	13.0
0.49	37	17.2	45	28.5	44	25.3	44	24.9	40	19.2
0.499	41	18.8	52	35.1	49	31.1	48	29.5	44	22.3
0.4999	43	19.6	60	39.6	59	38.8	54	33.2	48	24.5
0.49999	46	20.2	72	53.9	69	54.2	59	36.5	52	26.3
METIS decompositions										
0.3	36	13.1	39	15.2	37	14.0	38	14.6	36	13.1
0.49	42	19.4	52	30.3	50	27.0	48	27.7	44	22.2
0.499	47	24.1	58	39.9	56	35.6	56	35.7	50	27.9
0.4999	50	26.4	65	46.6	62	41.2	62	41.2	54	31.6
0.49999	56	28.6	73	51.1	69	44.5	68	44.8	60	33.8

subdomains. Math. Comp. **85** (299), 1085–1111 (2016).

[8] Chung, E.T., Kim, H.H., and Widlund, O.B.: Two-Level Overlapping Schwarz Algorithms for a Staggered Discontinuous Galerkin Method. SIAM J. Numer. Anal. **51**(1), 47–67 (2013).

[9] Dohrmann, C.R., Klawonn, A., and Widlund, O.B.: A family of energy minimizing coarse spaces for overlapping Schwarz preconditioners. In: U. Langer, M. Discacciati, D. Keyes, O. Widlund, and W. Zulehner (eds.) Proceedings of the 17th International Conference on Domain Decomposition Methods in Science and Engineering, held in Strobl, Austria, July 3-7, 2006, no. 60 in Springer-Verlag, Lecture Notes in Computational Science and Engineering, 247–254 (2007).

[10] Dohrmann, C.R., Klawonn, A., and Widlund, O.B.: Domain decomposition for less regular subdomains: Overlapping Schwarz in two dimensions. SIAM J. Numer. Anal. **46**(4), 2153–2168 (2008).

[11] Dohrmann, C.R. and Widlund, O.B.: An overlapping Schwarz algorithm for almost incompressible elasticity. SIAM J. Numer. Anal. **47**(4), 2897–2923 (2009).

[12] Dohrmann, C.R. and Widlund, O.B.: Hybrid domain decomposition algorithms for compressible and almost incompressible elasticity. Internat. J. Numer. Meth. Engrg. **82**, 157–183 (2010).

[13] Dohrmann, C.R. and Widlund, O.B.: An alternative coarse space for irregular subdomains and an overlapping Schwarz algorithm for scalar elliptic problems in the plane. SIAM J. Numer. Anal. **50**(5), 2522–2537 (2012).

[14] Dohrmann, C.R. and Widlund, O.B.: An iterative substructuring algorithm for two-dimensional problems in H(curl). SIAM J. Numer. Anal. **50**(3), 1004–1028 (2012).

[15] Dohrmann, C.R. and Widlund, O.B.: Lower Dimensional Coarse Spaces for Domain Decomposition. In J. Erhel, M. Gander, L. Halpern, G. Pichot, T. Sassi, and O.B. Widlund (eds.) Proceedings of the 21th International Conference on Domain Decomposition Methods in Science and Engineering, held in Rennes, France June 25–29 2012. no. 98 in Springer-Verlag, Lecture Notes in Computational Science and Engineering, 527–535 (2014).

[16] Dohrmann, C.R. and Widlund, O.B.: A BDDC algorithm with deluxe scaling for three-dimensional H(curl) problems. Comm. Pure Appl. Math. **69**, 745–770 (2016).

[17] Dryja, M., Sarkis, M.V., and Widlund, O.B.: Multilevel Schwarz methods for elliptic problems with discontinuous coefficients in three dimensions. Numer. Math. **72**, 313–348 (1996).

[18] Dryja, M., Smith, B.F., and Widlund, O.B.: Schwarz analysis of iterative substructuring algorithms for elliptic problems in three dimensions. SIAM J. Numer. Anal. **31**(6), 1662–1694 (1994).

[19] Galvis, J. and Efendiev, Y.: Domain decomposition preconditioners for multiscale flows in high-contrast media. Multiscale Model. Simul. **8**(4), 1461–1483 (2010).

[20] Graham, I.G. and Hagger, M.J.: Unstructured additive Schwarz-conjugate gradient method for elliptic problems with highly discontinuous coefficients. SIAM J. Sci. Comput. **20** (6),

2041–2066 (1999).
[21] Graham, I.G., Lechner, P.O., and Scheichl, R.: Domain decomposition for multiscale PDEs. Numer. Math. **106**(4), 589–626 (2007).
[22] Jones, P.W.: Quasiconformal mappings and extendability of functions in Sobolev space. Acta Math. **147** (1–2), 71–88 (1981).
[23] Karypis, G. and Aggarwal R. and Schoegel K. and Kumar V. and Shekhar, S.: METIS home page, http://glaros.dtc.umn.edu/gkhome/views/metis.
[24] Klawonn, A., Rheinbach, O., and Widlund, O.B.: Some computational results for dual-primal FETI methods for elliptic problems in 3D. Domain decomposition methods in science and engineering. Springer Lect. Notes Comput. Sci. Eng. **40**, 361–368 (2005).
[25] Klawonn, A., Rheinbach, O., and Widlund, O.B.: An analysis of a FETI–DP algorithm on irregular subdomains in the plane. SIAM J. Numer. Anal. **46**(5), 2484–2504 (2008).
[26] Klawonn, A., Widlund, O.B., and Dryja, M.: Dual-primal FETI methods with face constraints. Recent developments in domain decomposition methods (Zürich, 2001). Springer Lect. Notes Comput. Sci. Eng. **23**, 27–40 (2002).
[27] Klawonn, A. and Widlund, O.B.: Dual-Primal FETI methods for linear elasticity. Comm. Pure Appl. Math. **59** (11), 1523–1572 (2006).
[28] Kong, F. and Cai, X.-C.: A highly scalable multilevel Schwarz method with boundary geometry preserving coarse spaces for 3D elasticity problems on domain with complex geometry. SIAM J. Sci. Comput. **38** (2), C73–C95 (2016).
[29] Nečas, J.: Les méthodes directes en théorie des équations elliptiques, *Academia*, Prague, (1967).
[30] Nečas, J. and Hlavácek, I.: Mathematical Theory of Elastic and Elasto-Plastic Bodies: An Introduction, *Elsevier Scientific Publishing Co.*, (1980).
[31] Nitsche, J.A.: On Korn's second inequality. RAIRO Anal. Numér. **15**(3), 237–248 (1981).
[32] Oh, D.-S.: An overlapping Schwarz algorithm for Raviart-Thomas vector fields with discontinuous coefficients. SIAM J. Numer. Anal. **51**(1), 297–321 (2013).
[33] Shepard, D.: A two-dimensional interpolation formula for irregularly-spaced points. Proceedings of the 1968 ACM National Conference. 517–524, (1968).
[34] Sierra Structural Dynamics Development Team: Sierra Structural Dynamics – User's Notes. Technical Report SAND2016-9658, Sandia National Laboratories, 2016.
[35] Smith, B.F., Bjørstad, B.E., and Gropp, W.: Domain Decomposition: Parallel Multilevel Methods for Elliptic Partial Differential Equations, *Cambridge University Press, New York,* 1996.
[36] Toselli, A. and Widlund, O.B.: Domain Decomposition Methods - Algorithms and Theory, *Springer Series in Computational Mathematics*, **34**. Springer-Verlag, Berlin Heidelberg New York (2005).
[37] Van lent, J., Scheichl, R., and Graham, I.G.: Energy-minimizing coarse spaces for two-level Schwarz methods for multiscale PDEs, Numer. Linear Algebra Appl. **16**, 775–799, (2009).
[38] Xu, J.: Counterexamples concerning a weighted L^2 projections. Math. Comp. **57** (196), 563–568, (1991).